Int. J. High Technology Ceramics 3 (1987) 129–141

Examination of Carbon Inclusions in Sintered Silicon Carbide

R. Hamminger,* G. Grathwohl and F. Thümmler

Universität Karlsruhe, Institut für Werkstoffkunde II, Kernforschungszentrum Karlsruhe, Institut für Material- und Festkörperforschung, Postfach 3640, D-7500 Karlsruhe, FRG

SUMMARY

Particles of excess carbon are a general feature in the microstructure of sintered SiC. This phenomenon was studied by high resolution Auger electron spectroscopy on UHV-exposed fracture surfaces of (B, C)- and (Al, C)-doped materials. Normally the inclusions are about 1–2 μm in diameter, but particles of about 10–20 μm are also observed. The inclusions contain free carbon or carbon together with significant accompanying elements and phases, which were found to be characteristic for each particular material. The analytical results are briefly discussed with respect to processing and their impact on materials properties.

1 INTRODUCTION

Pressureless sintering of SiC involves the use of special sintering additives. Most practicable are B and C,[1,2] Al and C,[3–5] or even B, Al and C. Although several proposals have been made in order to explain the means by which these additives activate sintering, no unambiguous theory about the effective sintering mechanism has so far been established. Explanations in the case of (B, C)-doping deal with solid state sintering, accelerated by the increase of the surface to grain boundary energy ratio[6,7] due to the doping. Alternatively, the occurrence and assistance of a liquid phase,[8] at least at high B-concentrations, was also suggested.[9] The formation of grain

* Present address: Hoechst AG, Keramikforschung G864, Postfach 80 03 20, D-6230 Frankfurt 80, FRG.

Int. J. High Technology Ceramics 0267-3762/87/$03·50

boundary phases consisting of B_nC_m or $B_nC_m + C$ was also proposed,[10] but could not be confirmed by microanalytical investigations of the present authors.[11] In fact, both processes of solid state and liquid phase sintering may be active and may superimpose. Though there is very little known about the efficiency of the Al additions in the case of (Al, C)-doping, it may be suggested that Al enhances the sinterability by increasing volume diffusion. However, the addition of carbon as graphite or pyrolysed resin was found to be necessary in both methods of processing irrespective of the type of doping, i.e. B or Al. The role of carbon in densification is commonly explained by the deoxidation of the starting powders. In fact, the sintering process in SiC controlled by the additives is very complex and more detailed microanalytical information could be helpful for identification of effective mechanisms.

It is the aim of this investigation to describe the microstructural features and to analyse the chemical composition of excess carbon in sintered SiC (SSC) materials. Since the state of the grain boundaries is known in principle,[11] and the inhomogeneous microstructural distribution of B, Al and the impurity elements was discussed earlier,[12] the appearance of excess carbon has to be described in more detail for better understanding and evaluation of SSC materials.

2 MATERIALS AND EXPERIMENTAL METHOD

Five (B, C)- and two (Al, C)-doped SSC materials have been examined. These high quality and high density materials were produced by suppliers in Germany, the USA and Japan. All materials investigated were α-SSC with high values of the 4H- and 6H-polytypes in the case of (B, C)- and (Al, C)-

TABLE 1
Characteristics of the Investigated SSC Materials

Material	*Sintering additives*	*Fraction of theoretical density/%*	*Average grain size μm*	*Total content C_{free}/wt%*
SSC I	B,C	97·4	3·7	0·7
SSC II	B, C	98·2	4·5	0·6
SSC III	B, C	96·1	4·6	0·8
SSC IV	B, C	98·0	5·6	0·5
SSC V	B, C	93·3	3·7	1·1
SSC VI	Al, C	96·8	3·4	0·5
SSC VII	Al, C	96·1	3·5	0·6

doping, respectively. The values of density and average grain size are given in Table 1. Grain growth during sintering in inert atmospheres was controlled, and no exaggerated grain sizes have been observed. The grain sizes on average differ from each other by a factor of less than two. Deoxidation of the starting powders has been performed by addition of pyrolysable resins, while the total concentrations of excess free carbon have been determined chemically (Table 1).

The analyses were performed by imaging high resolution Auger electron spectroscopy (HRAES) in combination with a UHV specimen fracture attachment to avoid any contamination. HRAES permits monolayer-sensitive analysis at an optimum lateral resolution of about 50 nm, and in a later stage of investigations even as good as about 30 nm. Reproducibility and detection sensitivity are in the range of 0·2–0·5 at% in the case of light elements. The accelerating voltage of the primary electrons was 10 kV; the vacuum was about 8×10^{-8} Pa. Quantification of the analysis was done using known elemental sensitivity factors.[13]

3 RESULTS

The first characteristic difference between the two types of materials, (B, C)- and (Al, C)-doped SSC, is the appearance and distribution of the inclusions. (Al,C)-doped SSC exhibits fewer and smaller inclusions than (B,C)-doped materials and the inclusions are of a more uniform size, about 1–2 μm in diameter. In the case of (B, C)-doping, agglomerates of more than 10 μm were often found. Certain areas were also observed in (B, C)-doped samples, where inclusions were even larger than 20 μm in diameter. The inclusions observed were analysed and found to consist of excess, i.e. residual, graphite. These investigations were performed by X-ray diffraction. Characteristic differences were found by HRAES with respect to accompanying elements and phases, as discussed in the following sections.

3.1 (B, C)-doped SSC

In (B, C)-doped SSC I, stoichiometric BN exists inside graphite-type inclusions. An example is given in Fig. 1 by point analysis, showing also a secondary electron image and an appropriate distribution map of N. The coincidence of the dark inclusion with the map is conclusive. Unfortunately, the distribution of boron could not be demonstrated owing to insufficient intensity. The detectable elements in the spectrum are limited to Si (resulting from the bulk), C, B and N. Quantitative measurements gave evidence of the

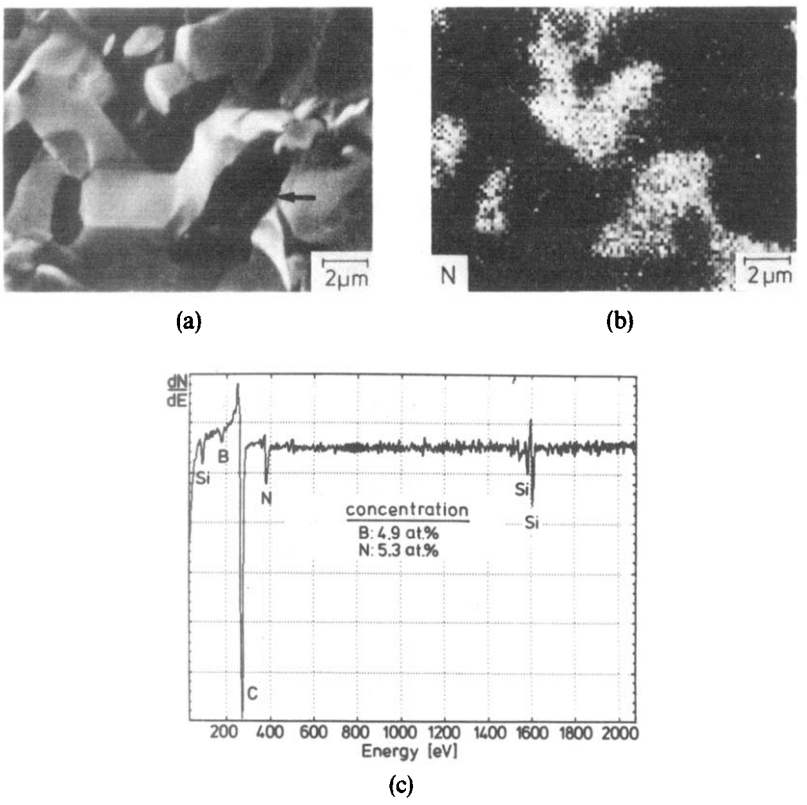

Fig. 1. HRAES point analysis of (B, C)-doped SSC I, indicating the existence of stoichiometric BN compounds inside graphite: a, SE image; b, N-map; c, HRAES point analysis in the marked area.

BN stoichiometry; the atomic concentrations were calculated[13] to be 4·9% B and 5·3% N.

(B, C)-doped SSC II exhibits two different types of C-containing inclusions. The first type was found to consist of pure graphite, homogeneously distributed and of uniform size. The second consists of B_4C, with no free C present. The example is presented in Fig. 2. It shows the secondary electron image (survey) and appropriate distribution maps of C and B. The point analysis inside the maximum brightness of the B-map evaluates atomic concentrations of 78·4% B and 20·7% C. Free B was not detected.

(B, C)-doped SSC III reveals inclusions of pure graphite. This is shown in Fig. 3 by secondary electron imaging and point analysis. No other elements or phases were observed.

The analysis of (B, C)-doped SSC IV is represented in Fig. 4. The secondary electron image and the appropriate distribution map of C

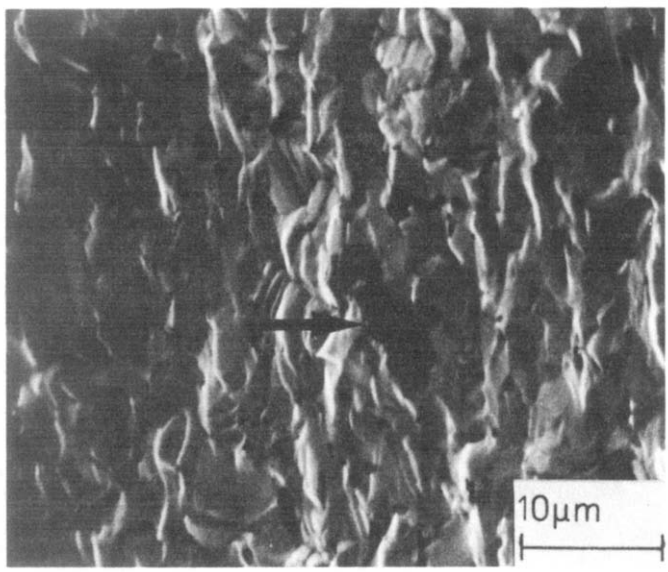

(a)

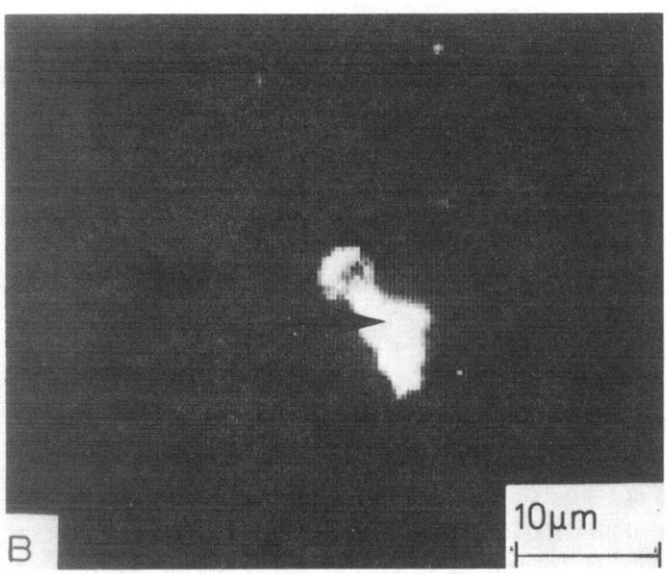

(b)

Fig. 2. HRAES point analysis of (B, C)-doped SSC II, indicating the existence of stoichiometric B_4C: a, SE image; b, B-map.

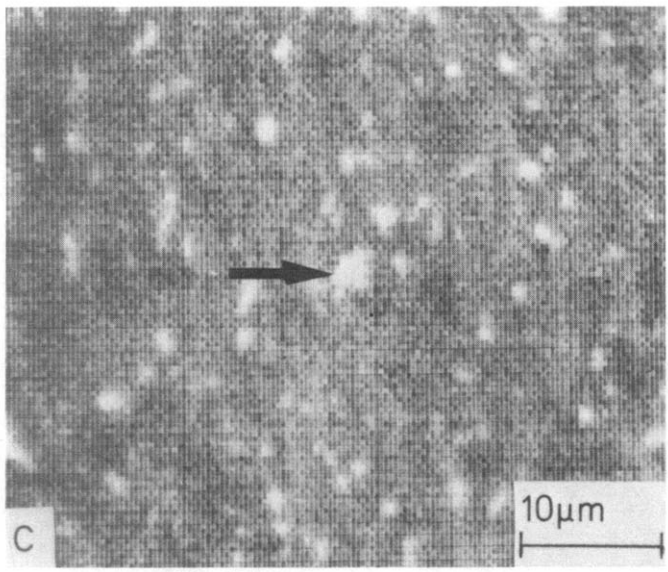

(c)

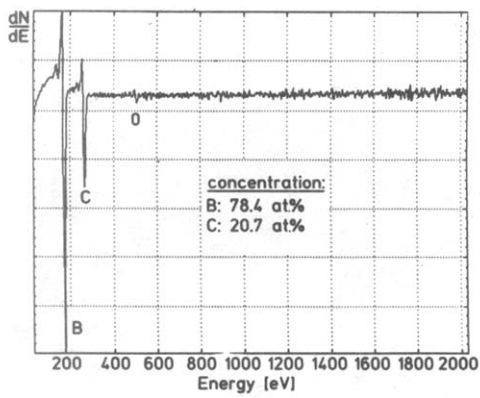

(d)

Fig. 2—*contd.* c, C-map; d, HRAES point analysis in the marked area.

correlate. The spectrum indicates the elements C, B and Si, the latter referable to the bulk material. The inclusions are graphite but contain some B, the concentration being about 3–4 at%. Precipitated B inside the graphite may be assumed to be present, as well as small portions of B_4C beside free C. B was no longer detected inside inclusions after a heat treatment of the material in ambient air (1500°C, 100 h).

(B, C)-doped SSC V was found to exhibit the highest concentration of excess C, compared to all other materials. The largest inclusions were also

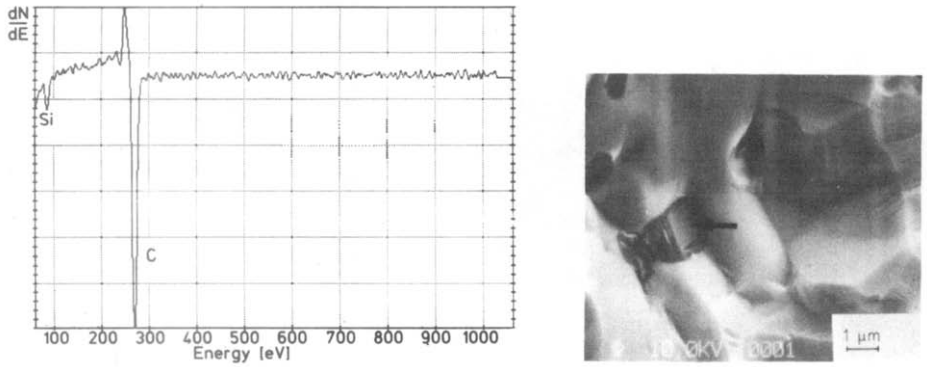

Fig. 3. HRAES point analysis of (B, C)-doped SSC III, indicating pure graphite.

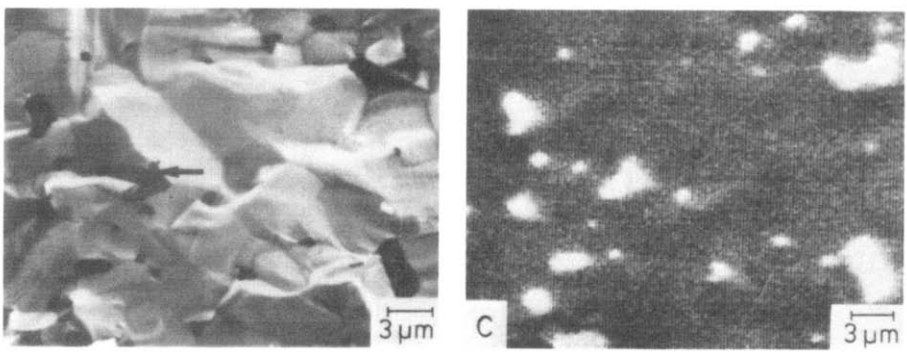

(a) (b)

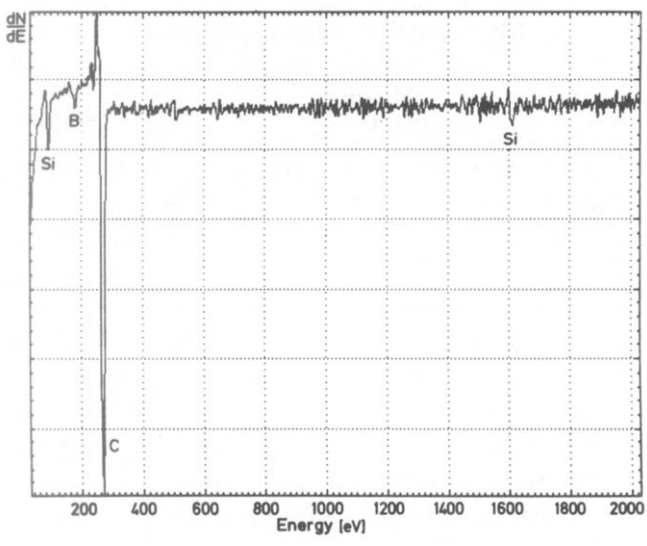

(c)

Fig. 4. HRAES point analysis of (B,C)-doped SSC IV, indicating traces of B inside graphite: a, SE image; b, C-map; c, HRAES point analysis in the marked area.

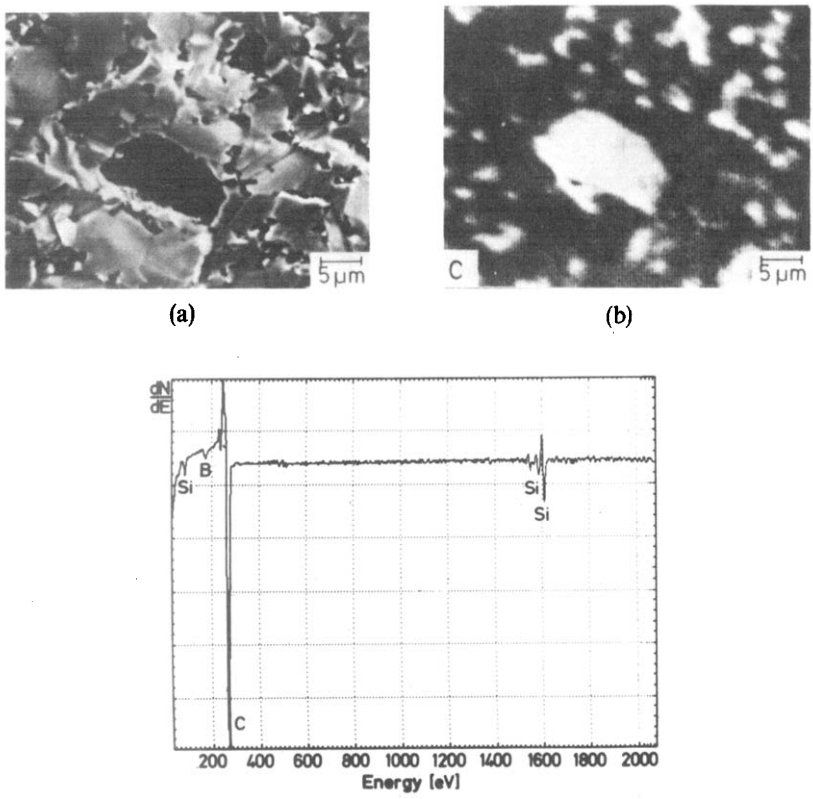

Fig. 5. HRAES point analysis of (B,C)-doped SSC V, indicating very high concentration of graphite and maximum-sized inclusions: a, SE image; b, C-map; c, HRAES point analysis in the marked area.

observed in this injection-moulded material. As a result of the analyses, inclusions of two types were found to exist side by side, similar to SSC II. Most inclusions consist of graphite, but some contain traces of B. This is demonstrated by point analysis in Fig. 5. It shows the secondary electron image, the appropriate distribution map of C and the HRAES spectrum of the marked region. The symmetry of the microstructure and C-map is clearly revealed. The spectrum indicates C and traces of B and Si. Both Si and B may originate from the matrix, the latter by reason of an inhomogeneous distribution and very high content.[11] Thus, the first mentioned inclusions are thought to be pure graphite, but inclusions of stoichiometric B_4C were confirmed by analysis next to pure graphite. Support of this argument is given in Fig. 6 by the secondary electron image, the appropriate distribution map of B and the point analysis inside its maximum brightness. The atomic concentrations have been calculated to be 77·6% B and 22·4% C.

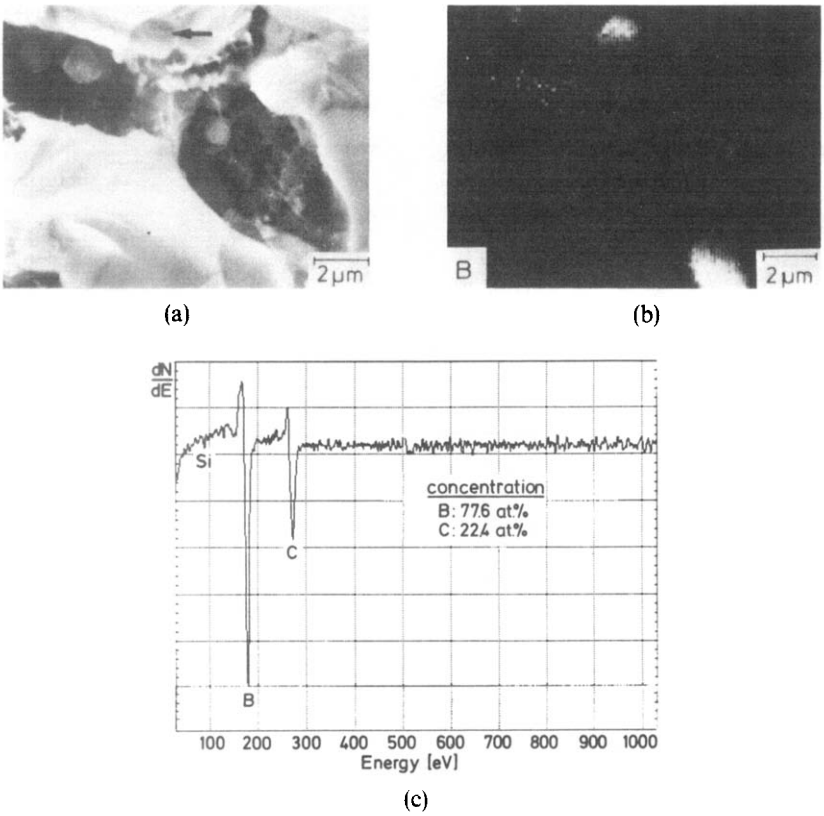

Fig. 6. HRAES point analysis of (B, C)-doped SSC V, indicating the existence of stoichiometric B_4C compounds next to graphite: a, SE image; b, B-map; c, HRAES point analysis in the marked area.

3.2 (Al, C)-doped SSC

Both (Al, C)-doped materials SSC VI and SSC VII reveal identical results. The inclusions of excess C are small in size and distributed rather homogeneously. Representative analyses are given in Figs 7 and 8. Figure 7 shows the secondary electron image, the appropriate distribution map of C and the point analysis of the marked inclusion in SSC VI. The graphite is accompanied by considerable contents of Al and Si, the latter most probably not originating from the matrix. Thus, the formation of Si–Al–C compounds inside free C inclusions is presumed. The line scan analysis through an inclusion of excess C is represented in Fig. 8 showing also the marked secondary electron image. When the particle is touched by the primary electron beam, an increase of the C-concentration and a decrease of the Si-concentration are clearly revealed. Again, Al was detected in this inclusion by point analysis, not shown here.

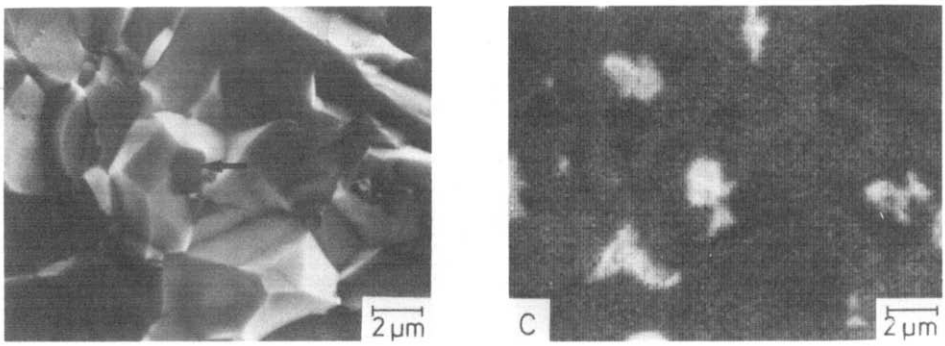

(a) (b)

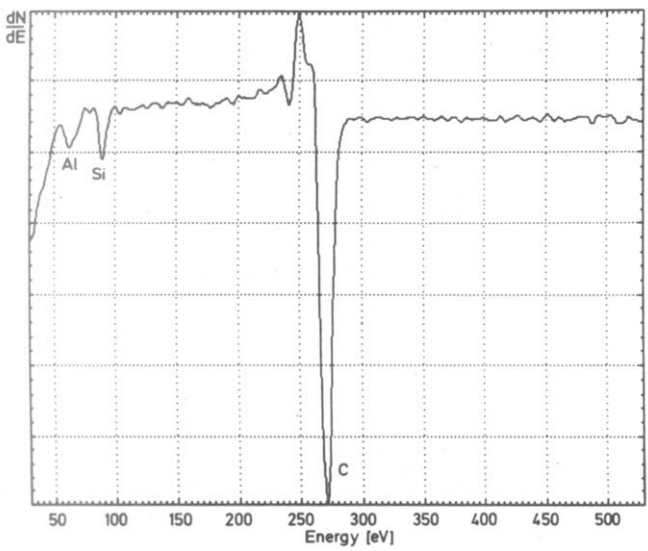

(c)

Fig. 7. HRAES point analysis of (Al, C)-doped SSC VI, indicating the presumed existence of Si-Al-C compounds beside graphite: a, SE image; b, C-map; c, HRAES point analysis in the marked area.

4 DISCUSSION

From studying fracture surfaces of SSC the most obvious fact is the general appearance of inclusions of excess carbon. Though this phenomenon was also observed elsewhere by means of analytical electron microscopy[5,14–16] and other methods,[17,18] there has so far been no detailed information about the chemistry of these inclusions. By means of HRAES, knowledge of the nature of these inclusions can be improved by the high lateral, as well as the

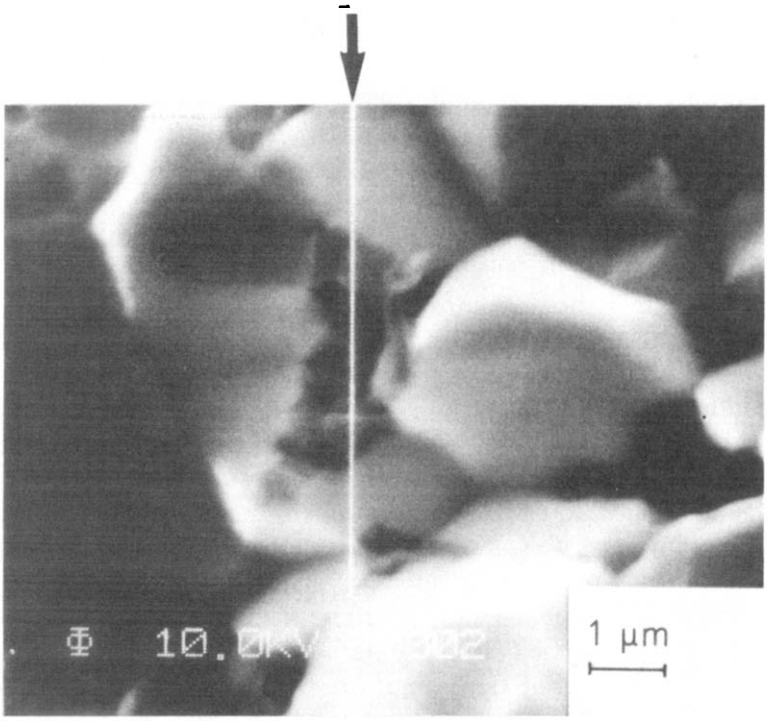

(a)

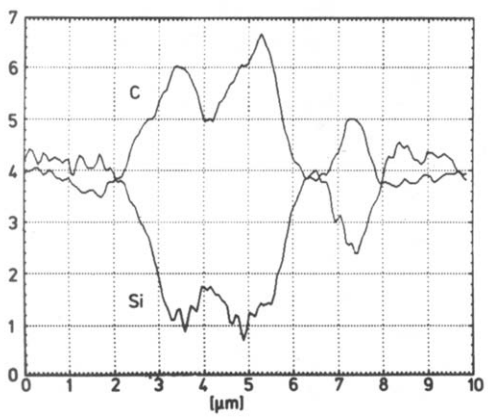

(b)

Fig. 8. HRAES line scan analysis through an inclusion of excess C in (Al,C)-doped SSC VI: a, SE image; b, line scan analysis.

spatial, resolution offered by this method. The analytical results have been obtained on sintered products. However, it can be assumed that equivalent agglomerates are also present in the powder compacts before sintering. The formation of particles as analysed in this study, and especially their distribution, raises a question about the processing procedure. The indication of the presence of BN and B_4C in (B, C)-doped materials is remarkable with respect to both the manufacturing procedure and the processes occuring during sintering; these compounds can possibly be formed during the sintering process but they could also be used as intentional additives. In any case it can be assumed that their efficiency during sintering is not optimized. The same is true with respect to the presumed existence of Si–Al-C-compounds inside the carbon inclusions, as measured in (Al, C)-doped SSC.

The influence of this free carbon on the mechanical properties of SSC, e.g. strength, has to be considered as detrimental, at least in principle. Although the commonly observed dimensions are small ($< 5\,\mu m$), the occurrence of agglomerates can lead to critical flaw dimensions. This effect may occur at room temperature as well as at high temperatures; however, a more detailed evaluation is only possible after further investigation.

Generally, the mechanical properties of SSC may be improved by increasing the homogeneity of the materials. Improved homogeneity means improved deoxidation of the primary powder particles, combined with a higher efficiency of the sintering additives, and diminishing of the number and size of free carbon inclusions in the final product.

REFERENCES

1. Prochazka, S., General Electric Co., *Dense silicon carbide ceramic and method of making same*, US Patent 3 852 099, 1974.
2. Prochazkam, S., Sintering of silicon carbide, in *Ceramics for High Performance Applications*, Eds J. J. Burke, A. E. Gorum and R. N. Katz, Brook Hill Publishing Co., Chestnut Hill, MA, USA, 1974, 239–52.
3. Böcker, W., Landferman, H. and Hausner, H., Sintering of alpha silicon carbide with additions of aluminum, *Powder Met. Int.*, **11** (1979) 83–5.
4. Hausner, H., Pressureless sintering of non-oxide ceramics, in *Energy and Ceramics*, Ed. P. Vincenzini, Elsevier, Amsterdam, 1980, 582–95.
5. Schwetz, K. A. and Lipp, A., The effect of boron and aluminum sintering additives on the properties of dense sintered alpha silicon carbide, *Science of Ceramics*, **10** (1980) 149–58.
6. Prochazka, S., *The role of boron and carbon in the sintering of silicon carbide*, General Electric Co., Schenectady, New York, Rep. No. 74 CRD 186, 1974.
7. Prochazka, S., Sintering of silicon carbide, in *Mass Transport Phenomena in Ceramics*, Eds A. R. Cooper and A. H. Heuer, Plenum Press, New York, 1975, 421–31.

8. Lange, F. F. and Gupta, T. K., Sintering of SiC with boron compounds, *J. Am. Ceram. Soc.*, **59** (1976) 537–40.
9. Böcker, W. and Hausner, H., The influence of boron and carbon additions on the microstructure of sintered alpha silicon carbide, *Powder Met. Int.*, **10** (1978) 87–9.
10. Suzuki, H. and Hase, T., Some experimental considerations on the mechanism of pressureless sintering of silicon carbide, in *Factors in Densification and Sintering of Oxide and Non-Oxide Ceramics*, Eds S. Somiya and S. Saito, Gakujutsu Bunken Fukyu-kai, Okayama, Tokyo, 1979, 345–65.
11. Hamminger, R., Grathwohl, G. and Thümmler, F., Microanalytical investigation of sintered SiC, Part 1: Bulk material and inclusions, *J. Mat. Sci.*, **18** (1983) 353–64.
12. Hamminger, R., Grathwohl, G. and Thümmler, F., Microanalytical investigation of sintered SiC, Part 2: Study of the grain boundaries of sintered SiC by high resolution auger electron spectroscopy, *J. Mat. Sci.*, **18** (1983) 3154–60.
13. Davis, L. E., MacDonald, N. C., Palmberg, P. W., Riach, E. G. and Weber, R. E., *Handbook of Auger Electron Spectroscopy*, 2nd Edn, Eden Prairie, MN, USA, Physical Electronics Inds. Inc., 1976.
14. Tajima, Y. and Kingery, W. D., Grain-boundary segregation in aluminum-doped silicon carbide, *J. Mat. Sci.*, **17** (1982) 2289–97.
15. Bourdillon, A. J., Jepps, N. W., Stobbs, W. M. and Krivanek, O. L., An application of EELS in the examination of inclusions and grain boundaries of a SiC ceramic, *J. Microscopy*, **124** (1981) 49–56.
16. Rühle, M. and Petzow, G., Microstructure and chemical composition of grain boundaries in ceramics, in *Surfaces and Interfaces in Ceramic and Ceramic–Metal Systems*, Eds J. Pask and A. Evans, Plenum Press, New York, 1981, 167–74.
17. Davis, R. F., Lane, J. E., Carter, C. H., Bentley, J., Wadlin, W. H., Griffis, D. P., Linton, R. W. and More, K. L., Microanalytical and microstructural analyses of B and Al regions in sintered alpha-SiC, *Scanning Electron Miscoscopy*, **3** (1984) 1161–7.
18. More, K. L., Carter, C. H., Bentley, J., Wadlin, W. H., Lavanier, L. and Davis, R. F., Occurrence and distribution of boron-containing phases in sintered α-silicon carbide, *J. Am. Ceram. Soc.*, **69** (1986) 695–8.

Received 25 September 1986; revised version received 26 January 1987; accepted 19 March 1987